

# SURFACE CHARACTERISTICS AND CARBON DIOXIDE FLUXES IN A SUBURBAN AREA OF BALTIMORE, MD: A GIS BASED METHODOLOGY

Ben Crawford\*, C.S.B Grimmond\*, J. Hom<sup>†</sup>, B. Offerle,\*\* and D. Golub<sup>†</sup>

\*Indiana University, Bloomington, IN

\*\*Göteborg University, Göteborg, Sweden

<sup>†</sup>U.S. Forest Service, Northeast Research Station

## 1. INTRODUCTION

A large and ever increasing proportion of the world's populations live in urban areas. Currently nearly 50% of the world's population lives in urban areas and by the year 2030, this number could increase to 61%, over 5 billion people (UN 2004). Increases in urbanization result in considerable changes to surface land-cover and roughness. Changes in land-cover can significantly alter the radiative, thermal, and moisture properties of the surface (Grimmond and Souch 1994) while changes in roughness lead to changes in turbulence characteristics which affect transport and exchange between the surface and the atmosphere. These changes alter balances of surface-atmosphere fluxes of energy, water (H<sub>2</sub>O), carbon dioxide (CO<sub>2</sub>), and momentum, creating an 'urban climate' differing from the climate of the natural surroundings (Grimmond and Souch 1994).

In order to better understand the urban climate and predict effects of urbanization, an understanding of the role and significance of the urban surface is vital. Climatological and meteorological measurement and modeling studies all require the active surface to be defined and described in order to characterize the study site, provide input for numerical models, and to ensure spatial consistency between measured and modeled data. Geographic information systems (GIS) provide a powerful means to analyze and illustrate the complexity of the urban surface-atmosphere interface. The objective of this paper is to present a GIS based methodology to characterize and objectively sample and analyze the urban surface with respect to earth-atmosphere carbon dioxide fluxes ( $F_{CO_2}$ ) (exchanges of carbon between the surface and the atmosphere). The methodology is illustrated with preliminary data from the AmeriFlux tower in the Cub Hill suburb of Baltimore, MD.

Urban areas are the primary source of carbon dioxide, a critical greenhouse gas, thus understanding the strength of cities of sources and sinks of CO<sub>2</sub> ( $F_{CO_2}$ ) has broad implications for global change research. Measuring and interpreting  $F_{CO_2}$  data collected in an urban environment presents several methodological challenges. The extreme spatial variability of land-cover and roughness elements typical of urban areas makes siting equipment to ensure representative measurements challenging (Grimmond et al. 2002). If the integrated flux of a neighborhood or a city is of interest, instruments need to be mounted on tall towers in areas of fairly uniform surface cover, so that observations are not unduly biased by roads, parks etc. The heterogeneous surface also makes interpretation of  $F_{CO_2}$  difficult in terms of measuring local CO<sub>2</sub> sources and sinks. In urban climatological/meteorological research, three spatial scales (micro-, local-, and meso-) for urban areas are commonly recognized.

At the micro-scale ( $10^1$ - $10^2$  m), spatial differences in carbon dioxide exchange ( $F_{CO_2}$ ) occur in response to building dimensions and orientations, land-cover, and proximity to  $CO_2$  emission sources. At the local-scale ( $10^1$ - $10^4$  m),  $F_{CO_2}$  represents the integrated response of an array of buildings, vegetation, and paved surfaces – characteristics of a neighborhood. Meso-scale ( $10^4$ - $10^5$ ) measurements consider the entire city and its differentiation from its surrounding areas (forest, agriculture, etc.) (Grimmond et al. 2002).

When studying  $F_{CO_2}$ , variations in vegetation cover and emissions from fixed (industrial or commercial) and mobile (traffic) sources are particularly important. In simplified terms, fossil fuel consumption and vehicular engine combustion add  $CO_2$  to the atmosphere while photosynthetic activity from vegetation removes  $CO_2$  from the atmosphere. In summertime in residential neighborhoods, in particular, irrigation (sprinklers used to water lawns, parks, gardens, etc.) is also important in controlling photosynthesis and thus carbon uptake by vegetation (Grimmond et al. 2002). The surface area affecting meteorological measurements of  $F_{CO_2}$  (i.e. the area for which the instruments are making measurements) is termed the ‘source area’ and is dependent primarily on the meteorological conditions at the time of observation (Schmid 1994). Since source areas are dynamic in nature, they vary with wind direction, speed and atmospheric stability, for example, they will have different surface characteristics at different. By linking  $F_{CO_2}$  data to the surface through the concept of source areas, it is possible to determine and objectively describe the surface influencing measurements at any particular time. Through GIS, dynamic source areas can be modeled and visualized both temporally and spatially. The source areas can also be integrated with spatially continuous surface datasets and point tower data and with appropriately stratified datasets. Thus GIS also makes possible surface analysis at a variety of scales.

## 2. METHODS

### 2.1 Study site

A 40.5 m tall tower located in the Cub Hill suburb ( $39.41^\circ N$   $76.52^\circ W$ ) of Baltimore, MD is mounted with instrumentation to continuously measure urban  $CO_2$  heat, water, and momentum fluxes between the surface and atmosphere. Turbulent flux instrumentation is mounted at 40.5 m oriented at approximately  $150^\circ$  and has been collecting data representative of the local-scale since May, 2001. Data are collected at 10 Hz and then processed in half-hour averages. The data presented here are from 2003. Other atmospheric variables such as air temperature, relative humidity, wind speed, wind direction, and precipitation are also measured at the site. The surrounding residential neighborhood is extensively forested (predominantly yellow poplar and oak hickory) and is primarily made up of one-story single-family homes. The area has also experienced recent increases in building and development that have resulted in land-cover changes that could affect  $F_{CO_2}$  measurements.

### 2.2 Surface database

In order to properly characterize and analyze the surface surrounding the tower, a surface GIS database must be developed at an appropriate scale and resolution. Care must be taken so that areal coverage is extensive enough while maintaining a sufficiently detailed spatial resolution. For data representative of the local-scale, a stratified dataset containing both local-scale and micro-scale data for the area of interest is appropriate. Also critical is what aspects of the surface

are meaningful for the process of interest, e.g. land-cover, land-use, building density, traffic density, etc. (Grimmond and Souch, 1994).

The primary dataset used for land-cover analysis was a vector polygon PAN/MSI image of the Cub Hill area of Baltimore, MD generated from IKONOS satellite imagery (Table 1). The image was orthorectified and projected in the Universal Transverse Mercator (UTM) zone 18 projection, NAD83 datum. Pixel size for this image was 1.00 m and land-cover was classified as road=1, water=2, tree=3, bare soil=4, grass=5, or building=6. Metadata concerning the methodology for land-cover classification were not provided. This polygon image was then converted to raster format at a cell size of 1 m based on land cover class. The image covers an areal extent of approximately 100 km<sup>2</sup> and is centered on the tower. LIDAR elevation and slope datasets at 0.5 m resolution for a 25 km<sup>2</sup> area centered on the tower were also analyzed. A polygon layer of building footprints covering the entire city of Baltimore was rasterized and clipped to fit the study area. Errors in these datasets depend on both the scale and resolution of classification and the classification strategies used. At the detailed resolution of analysis for this research, small spatial errors could have large impacts on results. For example, misclassification of land-cover types in a source area could lead to misinterpretation of observed F<sub>CO2</sub> measurements from that area.

Data	Extent	Resolution	Fields	Date	Source
Land-cover	10 km x 10km, centered on tower	1 m	road, water, tree, bare soil, grass, building	September, 2001	Space Imaging
Surface element elevation	~1 km x 1 km, centered on tower	0.5 m	easting, northing, elevation, intensity	February, 2002	CUERE, UMBC/BES
Surface elevation	~1 km x 1 km, centered on tower	0.5 m	easting, northing, elevation, intensity	February, 2002	CUERE, UMBC/BES
Slope	~1 km x 1 km, centered on tower	0.5 m	easting, northing, slope, intensity	February, 2002	CUERE, UMBC/BES
Building footprints	entire city, clipped to study area	1 m	area, perimeter, building ID	March, 1996	Baltimore County Office of Information Technology

**Table 1.** GIS dataset for Cub Hill flux tower. Dataset ordered from Space Imaging, Thorton, CO, ([www.spaceimaging.com](http://www.spaceimaging.com)). CUERE is the Center for Urban Environmental Research and Education at the University of Maryland, Baltimore County (UMBC). BES is the Baltimore Ecosystem Study, [www.beslter.org](http://www.beslter.org).

### 2.3 Source area calculations

Source areas are the dynamic link between surface data and meteorological data. They delimit the surface area influencing flux measurements. Conceptually (but not technically), source area models may also be thought of as the opposite of dispersion models; instead of modeling down-wind diffusion from a point source (the area over which pollutants are deposited), source areas are up-wind areas contributing to a point measurement. Since source areas are dynamic in nature, it is necessary to account for seasonal and diurnal patterns in F<sub>CO2</sub> during calculation. F<sub>CO2</sub> temporal patterns and magnitudes fluctuate from winter season to summer season and day and night based on vegetation respiration. The sign convention used here means that during summer, F<sub>CO2</sub> is positive at night (there is a net CO<sub>2</sub> exchange to the atmosphere) and then becomes negative during daylight hours (as plant photosynthesis acts to uptake CO<sub>2</sub> from the atmosphere). During the winter, when there is no active plant photosynthesis F<sub>CO2</sub> remains positive throughout

the day. Because of these distinct seasonal and diurnal cycles, in this study eight source areas representative of different seasonal and diurnal conditions encountered at the site were calculated and analyzed.

Flux source areas were calculated using Schmid’s (1994) scalar Flux-Source Area Model (FSAM). Generally, source area orientation is determined by wind direction, length by atmospheric stability, and width by a dispersion parameter. To illustrate the methodology presented here, a source area was calculated for each half-hour  $F_{CO_2}$  measurement for only neutrally stable conditions. Neutral conditions are often associated with moderate to strong surface winds, overcast skies, and little atmospheric heating or cooling from the surface. Half-hour source areas were then sorted by wind direction (primary or secondary, Figure 1), season (summer or winter, based on leaf cover), and time of day (day or night, based on incoming solar radiation). These sorted half-hour source areas were then averaged to create eight aggregate source areas (Table 2).

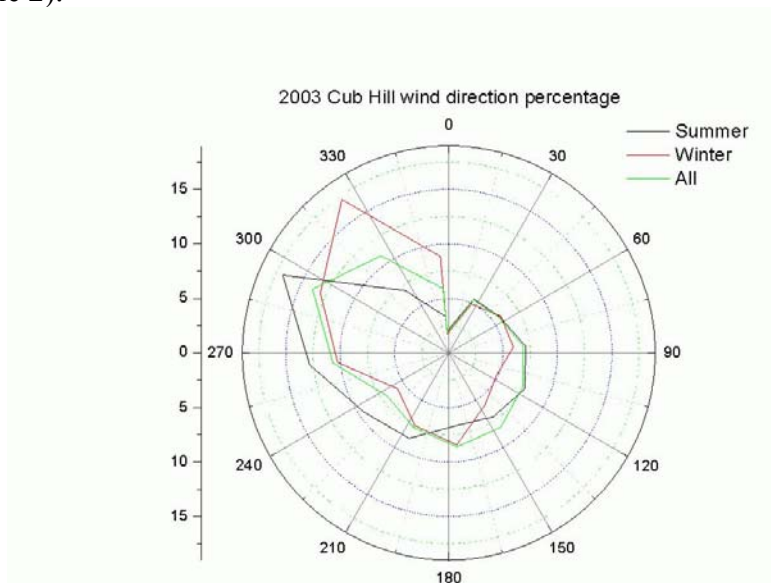


**Figure 1.** Baltimore wind rose, data are from 2003. Primary summer wind direction was 270-300° and secondary wind direction was 180-240°. Primary winter direction was 300-330° and secondary was 150-210°. Data are binned in 30° increments.

Source area name	Season	Time of Day	Wind Direction	n
SD1	Summer	Day	Primary	142
SD2	Summer	Day	Secondary	136
SN1	Summer	Night	Primary	82
SN2	Summer	Night	Secondary	61
WD1	Winter	Day	Primary	453
WD2	Winter	Day	Secondary	95
WN1	Winter	Night	Primary	31
WN2	Winter	Night	secondary	11

**Table 2.** Aggregate source areas for neutral conditions. Here summer was defined as periods with full leaf cover (days 129-287) and winter as periods with no leaf cover (days 1-93 and 324-365). Day or night was classified based on incoming solar radiation ( $K_{\downarrow}$ ). Periods with  $K_{\downarrow}$  less than  $25 \text{ W m}^{-2}$  were defined as night, periods with  $K_{\downarrow}$  greater than  $25 \text{ W m}^{-2}$  were defined as day. ‘n’ refers to the number of half-hour source areas averaged to create the aggregate source areas.

The output of the FSAM is an ASCII formatted, gridded, weighted elliptical area that corresponds to 90% of the area contributing to the measured flux (Figure 2). Each grid value is assigned a unique value weighted according to its probable contribution to the fluxes measured at the tower; cells located nearer to the tower generally contribute more to the flux. Only portions of source areas with grid cells contributing more than 0.1% to the total flux are displayed, and the preliminary results reported in this paper are based only on analysis of the highest 10% of weighted cells in the source area. In other words, the area with the highest 10% of weighted cells is the most important area contributing to the total  $F_{CO_2}$  measured for that time. All GIS operations, analysis, and results reported are for that small, but important fraction of the total source area (Figure 3). Unique cell values allow source areas to be analyzed at several different scales in the GIS. If a large portion or the entire source area is analyzed for this tower, this is representative of the local-scale, if the goal is to investigate the impact of specific, individual cells within the source area, this would be representative of the micro-scale.

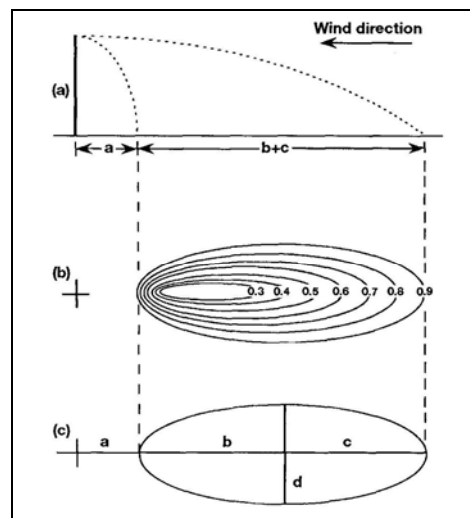


**Figure 2.** Elliptical source area output. a) side view b) plan view showing weighted ellipses, accounting for different percentages of influence on the measured flux. The largest ellipse accounts for 90% of the measured flux. c) plan view, here distance 'a' is shown as the distance from the tower to the beginning of the source area. (Grimmond 2001).

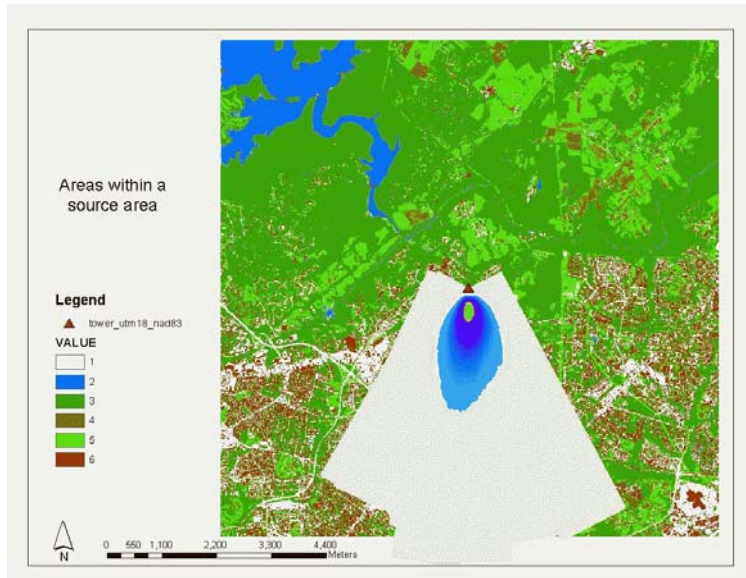


**Figure 3.** Areas within a source area. This is the source area for winter days during the secondary wind direction. The blue, purple, yellow and gray areas within the source area ellipse represent 90% of the measured flux. The gray area is made up of cells that contribute less than 0.1% of the measured flux. This is the least important part of the source area but makes up the greatest proportion of the area. Blue and purple areas represent cells that contribute greater than 0.1% and the yellow area is the highest weighted 10% of the source area. This area is most important to the measured flux - thus land-cover analysis was performed for this area. Land-cover values are 1: road, 2:water, 3: tree, 4: bare soil, 5: grass, and 6: building.

#### 2.4 GIS methods

Source areas, spatially continuous surface data, and point tower data are all integrated through the GIS. Source areas are imported into the GIS and overlaid on other surface datasets. Here visual representation can be manipulated, and surface analysis can be performed at a multitude of scales. Surface analysis with GIS was carried out in two main steps: (1) general surface description and characterization of the area surrounding the tower irrespective of source areas, and (2) surface description and characterization of the eight source areas. All analysis here is representative of the local-scale, the integrated response of an array of land-covers patterns, types, and functions on the point tower  $F_{CO_2}$  measurements. All GIS operations were performed with ArcGIS version 9 software (ESRI, ArcGIS 9). Percentage land-cover and average land-cover class heights were determined for a distance of 1 km from the tower using the clip and zonal analysis operations in ArcGIS. This analysis provided baseline local-scale observations of the surface surrounding the tower as well as provided initial estimates of roughness element heights into FSAM. Average height for each land-cover class was also determined by performing the zonal analysis operation on LIDAR elevation layers and land-cover layers. Building heights obtained from this method were unrealistic though (~2.0 m average building height), so the building polygon layer was used instead for the average building height. To do this, the building polygon layer was clipped to the size of the LIDAR elevation dataset and the zonal analysis operation was performed with the clipped building layer and elevation layer.

Source area analysis required further GIS manipulation since only a portion of the source area was of interest (Figure 3). After the source areas were imported into the GIS and oriented correctly, the area of interest needed to be clipped from the rest of the source area. To do this,

raster algebra was used to create a new raster set coded either 1 (area of interest) or 0 (area of non-interest). The areas of interest were then selected and a new layer was created from the selection. This layer with the exact shape of the area of interest was then used in the zonal analysis operation with land-cover and elevation datasets. These operations were all performed at the local-scale, but using a properly stratified and detailed surface dataset, source areas can be integrated with surface data and analyzed at the micro-scale. As different source areas from different time periods are imported into the GIS, temporal as well as spatial source area patterns can be analyzed.

#### 2.4.1 Surface Curvature

GIS was also used to calculate the degree of surface curvature (topography) around the tower and how this affects flux calculations. In order to calculate  $F_{CO_2}$  and other turbulent fluxes, three-dimensional wind speed and direction components must be realigned from the measurement reference frame into the reference frame of a chosen coordinate system (Finnigan 2004). The most commonly employed method of realignment, the 2-rotation method, involves defining coordinate rotation angles based on statistical properties of the mean wind direction. A newer method, however, the planar-fit method, uses an ensemble of mean wind vectors to define the coordinate rotation angles. In complex, steep topography, the planar-fit method is better in accounting for distorted wind vectors and is likely to yield much more stable results than the 2-rotation method (Finnigan 2004). If the topography is gentle, both the 2-rotation and planar-fit methods should work reasonably well (Finnigan, 2004). The purpose of these calculations is to determine the degree of wind vector distortion around the Cub Hill tower due to topography and whether the planar-fit method or the 2-rotation method is more appropriate for flux calculations.

Following the methodology outlined by Finnigan (2004), the tower footprint was estimated to be a circle with radius of  $10h$ , where  $h$  is the measurement height (40.5 m). Surface curvature was then estimated along the diameter of the footprint aligned with a primary wind direction. Surface curvature ( $R_o$ ) along this diameter was calculated from (Finnigan, 2004):

$$(10h)^2 = \left( \frac{(b - h_1) + (b - h_2)}{2} \right) \left( 2R_o - \left( \frac{(b - h_1) + (b - h_2)}{2} \right) \right)$$

where  $b$  is the tower base elevation (157.20 m), and  $h_1$  and  $h_2$  are the elevations at the ends of the diameter determined from the LIDAR elevation dataset. In order to test the robustness of the numbers and examine spatial variability around the tower,  $R_o$  was calculated for diameters every  $15^\circ$  from  $185^\circ$  -  $350^\circ$ . Since elevations were determined for each end of the diameter,  $R_o$  has in effect been calculated for every  $15^\circ$  around the tower (Figure 4).

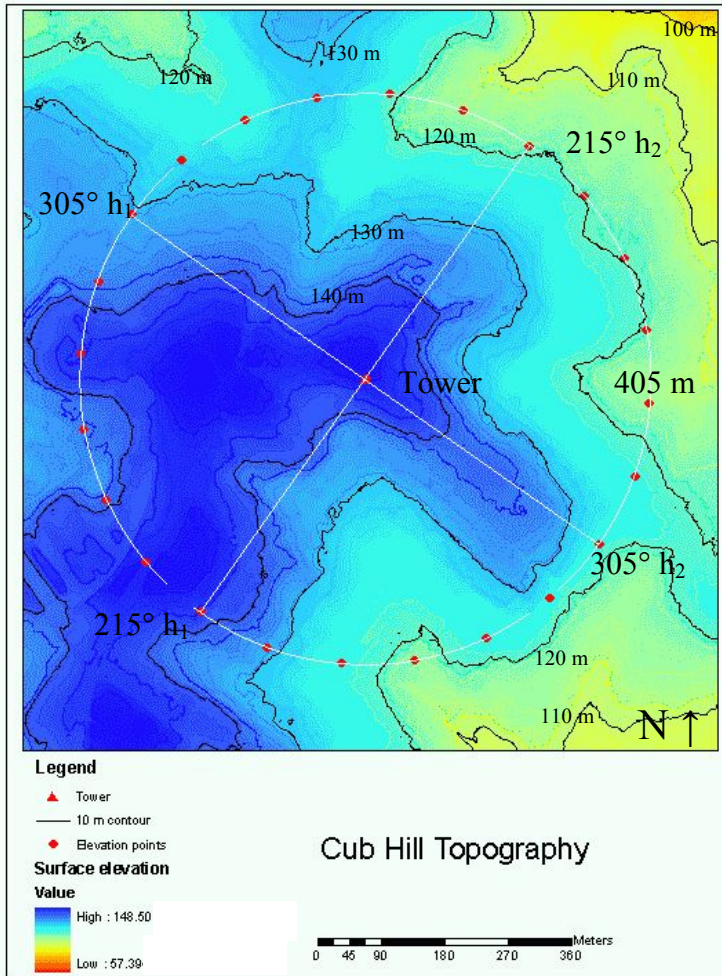


**Figure 4.** Points used to determine  $R_0$  and  $r_0$ . Circle radius is 405 m, elevations were estimated for each point shown; however only diameters and points for 305° and 215° are labeled. By convention, 0° is N, 90° E, 180° S, and 270° W.

### 3. PRELIMINARY RESULTS

#### 3.1 General surface characteristics

##### 3.1.1 General Composition

The most important land-cover classes in terms of  $F_{CO_2}$  are vegetated classes (trees and grass) and built-up classes (buildings and roads). Each of these classes affects  $F_{CO_2}$  differently. For vegetated surfaces,  $F_{CO_2}$  is negative during the day because of  $CO_2$  uptake by vegetation and positive at night due to vegetation respiration of  $CO_2$ . On the other hand, built surfaces have no mechanism (i.e. photosynthesis) to uptake  $CO_2$ , so on average  $F_{CO_2}$  always remains positive. The magnitude of  $F_{CO_2}$  from roads and buildings is a function of emissions and thus depends on traffic patterns, building energy consumption, and fossil fuel use. Over the course of a season or year, one would expect negative  $F_{CO_2}$  (net  $CO_2$  uptake by the surface) from vegetated surfaces and positive  $F_{CO_2}$  (net  $CO_2$  released to the atmosphere) from built-up surfaces. As mentioned before, the area surrounding the tower is extensively treed. Vegetated land-cover (tree or grass) makes up 70.97% of the total surface area, while built surfaces (roads and buildings) make up

27.42% of the total surface area (Table 3). In terms of  $F_{CO_2}$ , this means there will be large  $CO_2$  uptake by the surface in the summer months when vegetation's photosynthesis is most active. It remains to be seen if this uptake is large enough to offset  $CO_2$  production by industry and traffic in the area.

Land-cover class	% Cover
Road	13.18
Water	0.57
Tree	54.16
Bare soil	1.03
Grass	16.81
Building	14.24

**Table 3.** Land-cover (%) out to 1 km from flux tower.

As a preliminary analysis, land-cover (%) variability around the tower was examined by zonal analysis of  $30^\circ$  sectors out to 1 km around the tower (Figure 5). Trees covered the largest amount of land in every direction, ranging from 73.9% in the  $60-90^\circ$  sector down to 31.89% in the  $240-270^\circ$  sector. This latter sector also had the highest proportion of roads. Although  $F_{CO_2}$  varies by season,  $F_{CO_2}$  measured from these areas should be higher than from a more vegetated area because of less uptake by trees and more traffic emissions. Average height for each land-cover class was also determined (Table 4). Trees were the tallest surface elements with an average height of 11.43 m. Since vegetation height affects turbulence and wind velocity which affects both the magnitude of fluxes and source area shape, tree height data were used as an input for source area calculations.

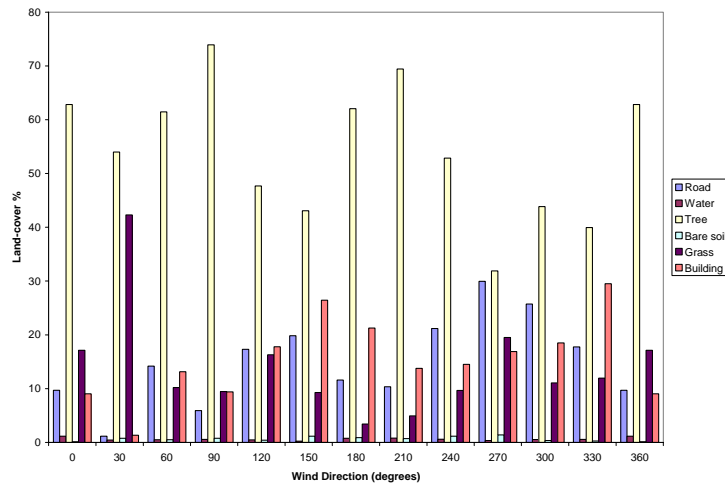


**Figure 5.** Land-cover proportions for  $30^\circ$  segments out to 1 km from the tower.

Land-cover class	Average height (m)
Road	1.76
Water	2.29
Tree	11.43
Bare Soil	1.30
Grass	0.95
Building	5.61

**Table 4.** Average land-cover class height for area surrounding the flux tower.

### 3.1.2 Surface Curvature

Surface curvature ( $R_0$ ) was determined for diameters every  $15^\circ$  from  $185^\circ$  -  $350^\circ$  based on estimated values of  $h_1$  and  $h_2$  at the ends of each diameter (Table 5). These numbers were then used to find values for  $h/(R_0+h)$  which were used to estimate the distortion of local streamlines due to surface curvature. For Baltimore, all  $h/(R_0+h)$  values are either 0.01 or 0.02. Since all values are approximately equal, flow distortion around the Cub Hill tower does not change greatly with wind direction, i.e. the relief around the tower is similar in all directions. These numbers are also smaller than values cited in the literature for other flux sites (Finnigan 2004). At the Tumbarumba, NSW, Australia site, for example, where  $h/(R_0+h) = 0.22$ , Finnigan states that “care must be taken in assessing advective effects” on fluxes. At the Griffin, Aberfeldy, Scotland site where  $h/(R_0+h) = 0.03$ , he suggests that the errors due to advective affects should be much smaller (Finnigan 2004).

Diameter ( $^\circ$ )	$h_1$ (m)	$h_2$ (m)	$\Delta h$ (m)	$R_0$ (m)	$h/(h+R_0)$
185	122.88	121.62	34.95	2364.04	0.02
200	131.70	115.70	33.50	2464.92	0.02
215	118.99	143.48	25.97	3171.56	0.01
230	146.48	119.38	24.27	3391.31	0.01
245	138.72	119.62	28.03	2939.90	0.01
260	136.62	119.10	29.34	2810.10	0.01
275	143.76	115.68	27.48	2998.35	0.01
290	136.64	122.63	27.56	2989.24	0.01
305	131.29	123.63	29.74	2772.52	0.01
320	127.60	123.51	31.65	2607.46	0.02
335	124.65	123.08	33.34	2476.92	0.02
350	129.10	117.33	33.98	2430.30	0.02

**Table 5.** Elevation,  $\Delta h$ ,  $R_0$  and  $h/(h+R_0)$  values.  $\Delta h$  values were calculated as the mean difference between the height of the tower base and the ends of each diameter,  $h_1$  and  $h_2$ . See Figure 4 for a visual representation of the points used for  $h_1$  and  $h_2$ .

The small values of  $h/(R_0+h)$  at Cub Hill indicate that flow distortion due to topography is weak and that the topography around the tower is gentle. Under these conditions, mean wind vectors are not distorted greatly so the 2-rotation method and the planar-fit method may be assumed to function equally well at determining coordinate rotation angles. This is an important finding for the meteorological work being conducted at the site.

### 3.2 $F_{CO_2}$ and land cover dynamics

In general, source areas during nighttime conditions were larger than their daytime counterparts (Table 6). It is important to note that only portions of the source area contributing more than 0.1% to the measured flux are displayed and here only the highest weighted 10% of the source areas are analyzed in terms of land-cover (Figure 6).

Source area name	Total area (km <sup>2</sup> )	Analysis area (km <sup>2</sup> )
SD1	1.25	0.016
SD2	0.44	0.049
SN1	3.44	0.063
SN2	6.11	0.118
WD1	2.39	0.038
WD2	1.75	0.055
WN1	5.61	0.097
WN2	2.23	0.139

**Table 6.** Source area areas. ‘Total area’ is the entire area of the source area, ‘Analysis area’ refers to the highest weighted 10% of cells contributing most to fluxes. This is the portion used for land-cover analysis. See Figure 3 for areas within a source area explanation.

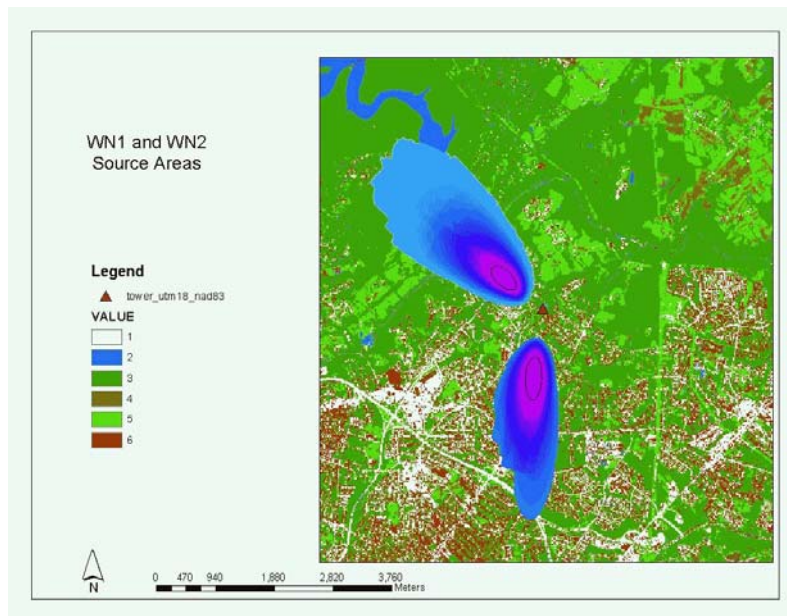


**Figure 6.** Example of source areas. WN1 and WN2 source areas are shown here, WN1 is the upper area, WN2 the lower area. The analyzed portions of source areas representing highest weighted 10% are outlined in black. The source area colors represent individual cell weighting, as the blue get darker, cells are weighted higher. The purple cells are weighted the highest.

Source area land-cover composition was also determined for each of the eight composite source areas (Figure 7). In terms of  $F_{CO_2}$ , it is expected that during the summer while there is active photosynthesis, vegetation cover is a strong control on  $F_{CO_2}$ . In simplified terms, because of tree respiration during the summer more trees will mean negative  $F_{CO_2}$  during the day and positive  $F_{CO_2}$  at night. Based on this hypothesis, daytime  $F_{CO_2}$  from SD1 should be less than from SD2 because of a higher percentage of trees in SD1. On the other hand, a larger percentage of trees in SN2 than SN1 indicates that nocturnal  $F_{CO_2}$  from SN2 should be higher than that from SN1. During the winter when tree respiration influences are negligible, source area differences in mobile and stationary  $CO_2$  sources will have the greatest impact. Source areas with large proportions of roads and homes, such as WD1, WN1, and WN2 may have higher  $F_{CO_2}$  values than source areas with comparatively low proportions. It remains to be seen if vehicle or

building CO<sub>2</sub> emissions have a greater impact on F<sub>CO2</sub> or at this site if lawn irrigation will enable vegetation to continue removing CO<sub>2</sub> from the atmosphere (thus lowering F<sub>CO2</sub>) throughout the winter. When there are no mitigating effects from vegetation to counteract human related emissions of CO<sub>2</sub> during the winter, other datasets such as traffic density and fossil fuel consumption need to be taken into account to explain source area differences in F<sub>CO2</sub>.

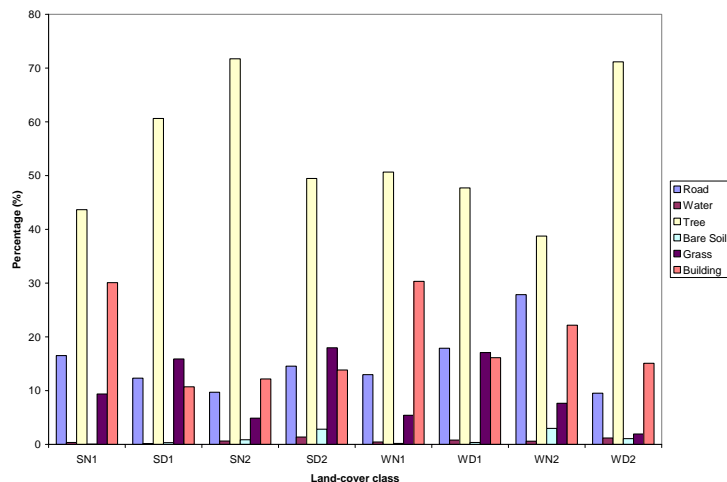


**Figure 7.** Land-cover composition of the eight source areas.

Land-cover resolution and classification errors could affect source area analysis results differently depending on the scale of analysis. At finer scales (e.g. micro-scale), classification errors could become magnified as ‘bad’ sections take up a disproportionate amount of the analysis surface. For example, at the micro-scale if an area that is truly a road is classified as vegetation, meaningful interpretation of F<sub>CO2</sub> becomes extremely difficult. As analysis scales become coarser (e.g. meso-scale), land-cover classification accuracy is still important, however classification errors may be canceled out by other errors or absorbed by the large analysis surface. The importance of resolution is also implied here, if the dataset resolution is too coarse, the scale of analysis must be limited to coarse scales. In order to perform meaningful analysis of source areas and F<sub>CO2</sub> at a number of scales, accurate datasets with high resolution are needed.

#### 4. CONCLUSIONS

GIS based methodologies are very useful in urban climate research. Methods outlined here demonstrate how to characterize, analyze, and sample the urban surface objectively and thoroughly with respect to F<sub>CO2</sub> at a variety of scales. The visualization, data integration, and analysis tools available in a GIS make source area imaging and analysis possible at a multitude of scales, provided surface datasets provide sufficient areal coverage and resolution. Topographical analysis of areas affecting flux measurements can also be performed. Preliminary results using the methodology outlined here show how source area land-cover makeup can be analyzed in detail and how topography affects both flux measurements and calculations. These both have significant impacts on interpretation of F<sub>CO2</sub> measurements, although more work needs to be done to analyze the sensitivity of these results to errors, especially in land-cover classification. Other future research could involve linking dynamic traffic flow data to the GIS or creating an F<sub>CO2</sub> surface based on urban surface parameterizations in order to study both

temporal and spatial  $F_{CO_2}$  patterns. Also, the database could be used to further understand the impact of surface topography and surface element height (i.e. vegetation and building height) on measurements from the flux tower and source areas. For example, source areas could be modified in an iterative process by which surface element heights are calculated for the source area, which are then entered as inputs to source area calculation thus changing the source area.

## 5. ACKNOWLEDGEMENTS

This research was funded by the United States Department of Agriculture, Forest Service Cooperative Research Agreement Award 03-CA-11242343-082, and the National Science Foundation, grant # BCS-0095284. I would also like to thank the co-authors, the USDA Forest Service personnel responsible for the day to day operation of the Baltimore flux tower, as well as Mike McGuire of UMBC and Dr. Tom Evans of IU for GIS support.

## 6. REFERENCES

- Chapman, L. and J. E. Thornes (2003). "The use of geographical information systems in climatology and meteorology." Progress in Physical Geography 27(3): 313-330.
- Finnigan, J.J. (2004). "A re-evaluation of long-term flux measurement techniques. Part II: Coordinate Systems," Boundary-Layer Meteorology 113: 1-41.
- Grimmond, C.S.B., B. Offerle, J. Hom, and D. Golub (2001). Poster: CO<sub>2</sub> and heat flux observations in suburban Baltimore (Cub Hill). Conference Proceedings, Ameriflux Convention, 2001.
- Grimmond, C. S. B., King, T.S., Cropley, F.D., Nowak, D.J., Souch, C. (2002). "Local-scale fluxes of carbon dioxide in urban environments: methodological challenges and results from Chicago." Environmental Pollution 116: S243-S254.
- Grimmond, C.S.B. and C. Souch (1994). "Surface Description for urban climate studies: a GIS based methodology." Geocarto International 1: 47-59.
- Jo, H.-K. and E.G. McPherson (1995). "Carbon storage and flux in urban residential greenspace." Journal of Environmental Management 45: 109-133.
- Jo, H.-K. and E.G. McPherson (2001). "Indirect carbon reduction by residential vegetation and planting strategies in Chicago, USA." Journal of Environmental Management 61: 165-177.
- Jo, H.-K. (2002). "Impacts of urban greenspace on offsetting carbon emissions for middle Korea." Journal of Environmental Management 64: 115-126.
- McPherson, E. G. (1998). "Atmospheric carbon dioxide reduction by Sacramento's urban forest." Journal of Arboculture 24: 215-223.
- Moriwaki, R., and M. Kanda (2004). "Seasonal and diurnal fluxes of radiation, heat, water vapor, and CO<sub>2</sub> over a suburban area." submitted for publication: Journal of Applied Meteorology.
- Nemitz, E., K.J. Hargreaves, A.G. McDonald, J.R. Dorsey, and D. Fowler (2003). "Micrometeorological measurements of the urban heat budget and CO<sub>2</sub> emissions on a city scale." Environmental Science and Technology.
- Oke, T.R. (1984). Methods in urban climatology. In: Kirchofer, W., Ohmura, A., Wanner, W. (Eds.), Applied

climatology. Zurcher Schriften 14, ETH, Zurich, pp. 19-29.

Scherer D., U. F., H.-D. Beha, and E. Parlow (1999). "Improved concepts and methods in analysis and evaluation of the urban climate for optimizing urban planning process." Atmospheric Environment 33: 4185-4193.

Schmid, HP (1994). "Source areas for scalars and scalar fluxes." Boundary-Layer Meteorology, 67(3): 293-318.

Soegaard, H., and L. Moller-Jensen (2003). "Towards a spatial CO<sub>2</sub> budget of a metropolitan region based on textual image classification and flux measurements." Remote Sensing of Environment 87: 283-294.

Takagi, M., K. Gyokusen, and A. Saito. (1998). "Increase in the CO<sub>2</sub> exchange rate of leaves of *Ilex rotunda* with elevated atmospheric CO<sub>2</sub> concentration in an urban canyon." International Journal of Biometeorology 42: 16-21.

Takahashi, H. A., Hiyama, T., Konohira, E., Takahashi, A., Yoshida, N., Nakamura, T. (2002). "Diurnal variation of CO<sub>2</sub> concentration, D14C and d13C in an urban forest: estimate of the anthropogenic and biogenic CO<sub>2</sub> contributions." Tellus 54B: 97-109.

U.N. 2004. [www.un.org/esa/population/pubsarchive/ura/fura.htm](http://www.un.org/esa/population/pubsarchive/ura/fura.htm), accessed March 3, 2004.

Vogt, R., M.W. Rotach, M. Roth, A.N.V. Satyanarayana (2003) "Fluxes and profiles of CO<sub>2</sub> in the urban roughness sublayer." Conference Proceedings, International Conference on Urban Climate; Łódź, Poland, 2003.

Wilhelmi, O. V. and J. C. Brunskill (2003). "Geographic information systems in weather, climate, and impacts." Bulletin of the American Meteorological Society: 1409-1414